CrystEngComm

Accepted Manuscript

ROYAL SOCIETY OF CHEMISTRY

www.rsc.org/crystengcomm

Table of Contents

'Honeycomb' nanotube assembly based on thiacalix[4]arene derivatives by weak interactions

Wei Wang[a], Weiping Yang[a,b], Rong Guo[a] and Shuling Gong[a,*]

[a] *College of Chemistry and Molecular Sciences, Wuhan University, Wuhan 430072, PR China*

[b] *Key Laboratory of Tobacco Flavor Basic Research, Zhengzhou Tobacco Research Institute of CNTC, No. 2, Fengyang Street, High-Tech Zone, 450001 Zhengzhou, China*

**Corresponding Author: E-mail: gongsl@whu.edu.cn; Fax: +86 27 68754067; Tel: +86 27 68752701.*

Crystallisation of six thiacalix[4]arene derivatives from hexane-chloroform leads to 'honeycomb' nanotube architectures and each tubular stack is sounded by six close neighbours tubular *via* weak interactions, such as S···π interaction, C-H···π interactions, and so on.

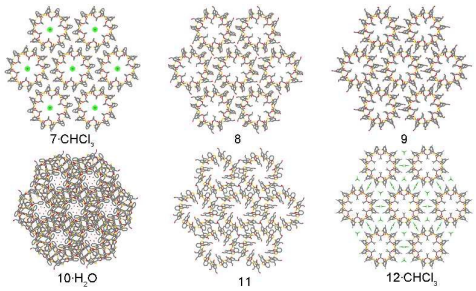

Cite this: DOI: 10.1039/c0xx00000x

www.rsc.org/xxxxxx

ARTICLE TYPE

‘Honeycomb’ nanotube assembly based on thiacalix[4]arene derivatives by weak interactions

Wei Wang,[a] Weiping Yang,[a,b] Rong Guo[a] and Shuling Gong[a,]*

Received (in XXX, XXX) Xth XXXXXXXXX 20XX, Accepted Xth XXXXXXXXX 20XX

DOI: 10.1039/b000000x

The crystal structures of di-O-Propoxy-mono-Formyl-thiacalix[4]arene·chloroform (**7·CHCl$_3$**), di-O-Propoxy-di-Formyl-thiacalix[4]arene (**8**), di-O-Propoxy-tri-Formyl-thiacalix[4]arene (**9**), di-O-Benzyol-di-Formyl-thiacalix[4]arene·water (**10·H$_2$O**), mono-O-Propoxy-tri-Formyl-thiacalix[4]arene (**11**), di-O-Propoxy-di-Cyano-thiacalix[4]arene·chloroform (**12·CHCl$_3$**) in the same crystallisation medium have been investigated. These crystals form similar ‘honeycomb’ nanotubes architectures and display different assemblies in the solid state. **7·CHCl$_3$**, **8**, **9** and **11** assemble to ‘classical’ head-to-head dimer *via* interdigitation of aromatic rings with π···π stacking interactions, while **12·CHCl$_3$** form a novel head-to-head dimer motif and infinite network structures are stabilised by Cl···Cl, Cl···π and CN···Cl interactions. Although **10·H$_2$O** does not form head-to-head dimer, it has taken in a new cubic closest packing (ccp), forming a water channel nanotube. X-ray single-crystal diffraction studies reveal that the weak interactions, including C-H···O, halogen···halogen, C-H···π, lone pair (lp)···π and π···π interactions are contributing to the supramolecular assembly.

Introduction

Hollow tubular architectures of ring-shaped organic molecules, such as cyclopeptide,[1] crown ethers,[2] pyrogallol[4]arenes,[3] C-alkylresorcin[4]arenes[4] and calix[4]arene,[5] have attracted wide attention of chemists due to their great prospects in nanomaterials, selective guest encapsulation, biological channels and drug delivery. But it is difficult to control the self-assembly of macrocyclic molecules to form an infinite network structure, because that is often a compromise between the geometrical constraints of the building blocks and the competing weak intermolecular interactions.[4, 6]

Hydrogen bonding often play a key role in the self-assembly of molecules into an organised supramolecular structures.[5a, 7] On the other hand, a set of somewhat weaker interactions, including C-H···O,[8] C-H···S,[9] C-H···π,[10] cyano···halogen,[11] halogen···halogen,[12] lone pair (lp)···π,[13] and π···π interactions,[4, 14] not more than a few Kcal/mol also play an crucial role in supramolecular structures when stronger hydrogen bonding is absent.

Calixarenes,[15] which can be tailored by functionalising either the ‘lower rim’ or ‘upper rim’, has been extensively studied in the design of hexameric, dimeric capsules, bilayers or nanostructures. ‘Honeycomb’ nanotube[11] assembly of calixarenes can be obtained by hierarchical self-assembly:[16] first intermolecular aggregates form a closed disk-shaped oligomeric, and then aggregation of multiple disks into rods or cylinders objects through non-covalent interactions. Recently, Dalgarno *et al*.[5i] has reported that in the presence of pyridine (acting as a template), *p*-carboxylatocalix[4]arenes (**1**) has formed a head-to-head hydrogen-bonded dimer motif facilitated by host−guest interactions (Fig. 1B) and the six molecules form a specific hexameric disc through parallel back-to-back packing almost situated in the same plane (Fig 1C and 1D). The extend structure show that these dimers act as bridges form a ‘cog-like’ or ‘honeycomb’ architecture. The whole molecular crystallisation is stabilised by N-H···O, C-H···O, C-H···π and π···π interactions. The ‘honeycomb’ architecture gives rise to two channels: *endo*-channel (triply helical nanotubes) and *exo*-channel (interstitial space was created between adjacent nanotubes).

Thiacalixarenes,[17] the presences of four sulfur atoms instead of CH_2 groups, has many novel features compared with ‘classical’ calixarenes, which also can be used to form a range of structural motifs. Compared with a large number of ‘honeycomb’ nanotube studies available for ‘classical’ calixarenes, only a few number of thiacalixarenes, including di-propyl-thiacalix[4]arenes (**2**),[18] 1,3-*alt*-tetrabromo-tetrapropoxy-thiacalix[4]arene (**3**)[19] and 1,3-*alt*-tetrabromo-tetrabutoxy-thiacalix[4]arene (**4**)[20] could form such ‘cog-like’ architecture nanotube. Compound **2** can be assembled into a head-to-head dimer *via* interdigitation of aromatic rings with C-H···π and π···π interactions (Fig. 1E). Symmetry expansion of the crystal structure of **2** reveals that two trimeric units (three molecules of **2** are situated in the same plane) pack as a hexagonal close–packed (hcp) arrangement and C-H···S and S···π interactions assist with the stacking (Fig. 1F, 1G, 1H and Fig. S1, Supporting Information). The common head-to-head dimer motif is not observed in the crystal structure of **4**, and examination of the extended array shows that the infinite open network structures are stabilised by triangular Br_3 synthon-type halogen···halogen interactions (Fig. 1I)[12c] and S···π interactions. In these previous work[5, 18-21] we realised that 1) solvent molecules

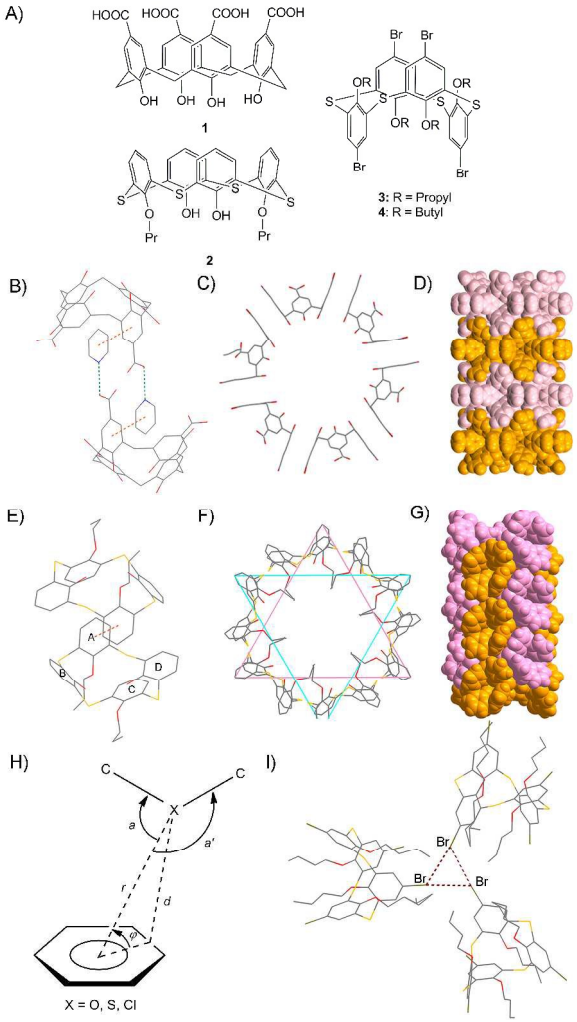

Fig. 1 (A) Schematic of calix[4]arenes **1**-**4**. (B) Pyridine templated dimerisation of **1**. (C) Back-to-back assembly of **1** to form hexameric discs. (D) Interlocked hexameric discs (orthogonal view to (C)) to form infinite nanotubes of **1** shown in alternating colour. (E) Host-to-host dimer assembly of **2**. (F) Back-to-back assembly of **2** to form hexameric discs. (G) Interlocked hexameric discs (orthogonal view to (F)) to form infinite nanotubes of **2** shown in alternating colour. (H) The parameters defining the geometry of lp···π interactions.[13c, 13e] (I) The triangular Br_3 synthon interaction in **4**.

and the backbone of calixarenes all play an important part in the construction of nanotube, 2) the interdigitated dimer motif is almost omnipresent.[5]

Our earlier work has reported that a one-dimensional channel formed by 1,2-*alt*-tetra-acetic acid calix[4]arene[21] and a three-dimensional network of *endo*-aquatubes formed by 1,3-*alt*-thiacalix[4]arene derivatives[22] are both stabilised by the strong intermolecular hydrogen bonding. In the present contribution, we have expanded our self-assembly studies with thiacalix[4]arene derivatives to explore the tolerance of the head-to-head dimer motif and 'honeycomb' architecture towards host molecule scaffolds alteration when stronger hydrogen bonding is absent. The modification consists in introducing different organic substituents either into aromatic rings or instead of protons of OH groups with the partial removal of active protons. We also studied their ability to stack by weak interactions, such as S···π, π···π

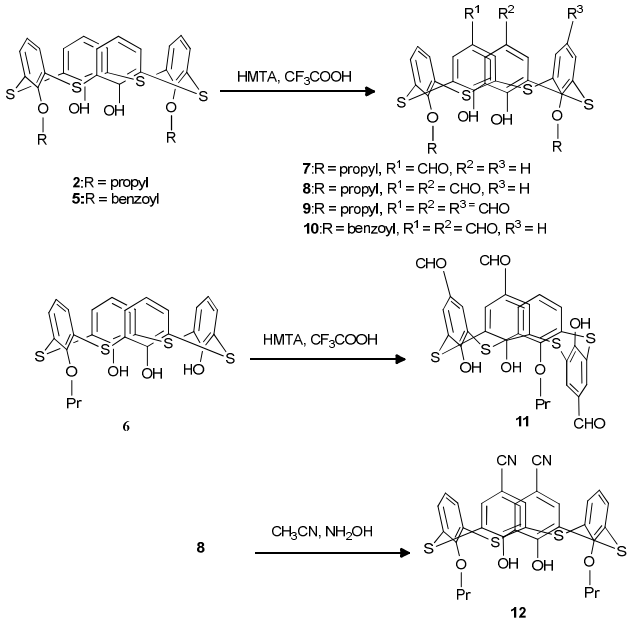

Scheme 1 Syntheses of the six compounds.

interactions and so on. Based upon the above, we have been prepared six thiacalix[4]arene derivertives **(7-12)** according to a known literature (Scheme 1).[17b,17c, 23] All compounds are soluble well in chloroform, so we employ hexane-chloroform as a solvent for crystallisation. Slow evaporation over several days at room temperature afford single crystals suitable for X-ray diffraction studies. The results of these crystallisation show that modest changes in the primary structure of thiacalix[4]arene lead to different packing in the solid state, but all compounds form the 'honeycomb' architecture which is stabilised by weak interactions (Fig.2).

Results and discussion

Crystal structure of 7· $CHCl_3$

Single crystals of **7·$CHCl_3$** are in a trigonal cell, and structure was performed in the space group $R\bar{3}$. The asymmetric unit consists of one molecule of **7** and one-sixth of the chloroform molecules which is disordered near the lower-rim propoxy groups. In the solid state, compound **7** adopts a cone conformation is due to O-H···O interactions and O-H···S interactions (Table S7, Supporting Information). The aromatic ring D is highly disordered over two positions, and the non-disordered situation is modelled at 85.9% with refined site occupation factors (Table S17). This positional disorder might be related to the interactions with solvent molecular: two weaker C-H···Cl interactions[13d] between hydrogen atoms of methyl or methylene groups attributed to propyl group of **7** and chlorine atoms with C(24)-H(24A)···Cl(1) and C(25)-H(25B)···Cl(2) distances of 2.86 Å and 2.99 Å (Fig. 3B). The values of the dihedral angles between the aromatic rings and the plane R (R defined as least squares plane passing through the S atoms)[22a] are equal to respectively (Table S2). Compared with compound **2**, the aromatic rings D is flipped inward approximately 7.3º, meanwhile other aromatic rings are flipped outward.

Within the asymmetric unit, two molecules of **7** to form a

Cite this: DOI: 10.1039/c0xx00000x

www.rsc.org/xxxxxx

ARTICLE TYPE

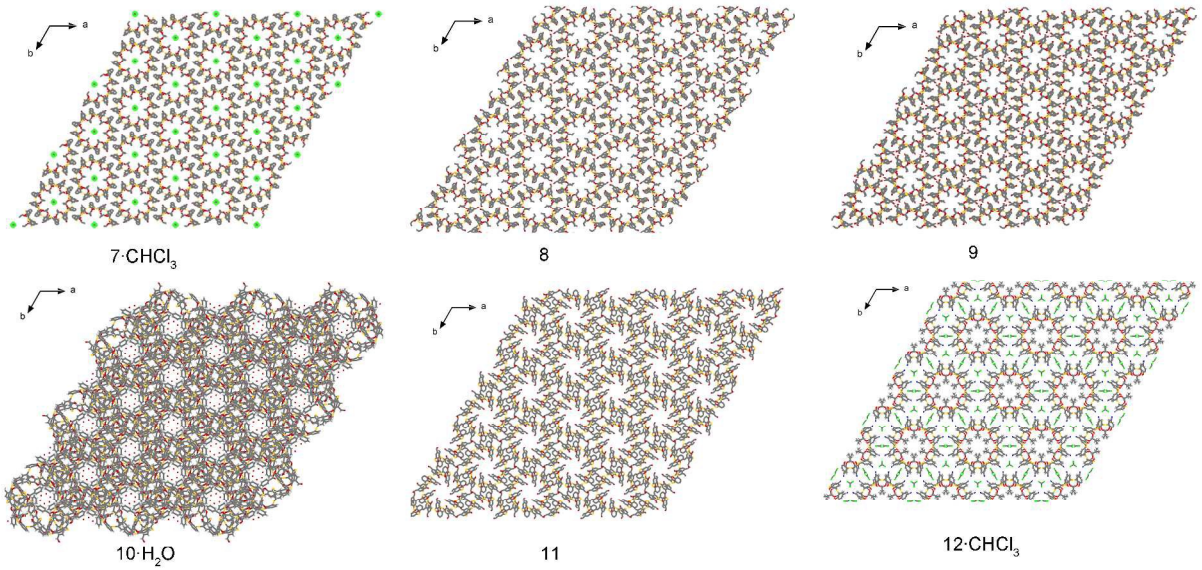

Fig. 2 Overall crystal structure of six compounds existing as a supramolecular assembly, view along the crystallographic *c* axis.

head-to-head dimer *via* π···π interactions between parallel aromatic ring A of the dimer with aromatic centroid distance of 4.050 Å (Table S4). Three weaker C-H···π interactions with symmetry unique C(3)-H(3)···aromatic centroid, C(4)-H(4A)···aromatic centroid and C(5)-H(5)···aromatic centroid distances of 3.183 Å, 3.179 Å and 3.123 Å are associated with the π···π interactions (Fig. 3A and Table S5). No C-H···O interaction is formed by the upper rim formyl group with adjacent dimer.

In the extended structure, the asymmetric unit forms a triply helical tube (Fig. S2). View along the crystallographic *c* axis, six molecules pack in a back-to-back parallel arrangement, similar to compound **2**, forming hexameric disc and a chloroform molecular resides the centre of the hexameric discs (Fig. 3B). View along the crystallographic *b* axis, there are three weaker C-H···π interactions with C(23)-H(23A)···aromatic centroid, C(7)-H(7A)···aromatic centroid and C(13)-H(13)···aromatic centroid distances of 2.93 Å, 2.77 Å and 3.138 Å, respectively. A weak C-H···O interaction between an aromatic ring proton of one molecule and a formyl group at the adjacent molecule with C(20)-H(20)···O(5) distance of 2.64 Å. Furthermore, C-H···S and S···π interactions are also observed in the triply helical tube. There are two C-H···S interactions with C(7)-H(7B)···S(2) and C(31)-H(31)···S(1) distances of 3.02 Å and 2.97 Å, respectively (Fig. 3B and 3C). In this case, the S···π interactions can be classified as Type III according to a report by Chong-Qing Wan.[13e] As is shown in Fig. 3C and Table S3, S(2) atom is embraced by two neighbouring aromatic rings. The distances from S(2) to the aromatic rings centre (*r*) are 4.357 Å and 4.150 Å, the closest aromatic ring edge (*d*) are 3.820 Å and 3.599 Å, the C(12)-S(2)···centroid (*α*) are 74.72º and 168.48º, C(17)-S(2)···centroid (*α'*) are 154.99º and 71.26º, and C(6) / C(30)-centroid-S(2) (*φ*) are 58.42º and 57.52º. Similar to S(2) atom, S(4) atom also forms a bent sandwich geometry, and the detail metric parameters are listed in Table S3.

Neighbouring hexameric tubes form a 'honeycomb' architecture which is stabilised by the weak interactions (Fig. 3D and 3E, π···π, C-H···π interactions in the dimer have already been described in Fig. 3A). Additionally, there are two weaker C-H···O interactions with C(21)-H(21)···O(5) and C(22)-H(22)···O(5) distances of 2.47 Å and 2.60 Å (Fig. S3). The distance between adjacent nanotubes is 21.34 Å and a complete cycle contains six host molecules with distance of 35.45 Å (Table 1).

Crystal structure of 8

Guest-free crystals of **8** were obtained as colourless block crystals in the trigonal space group $R\bar{3}$. The asymmetric unit is composed of one molecule of **8** stabilised in a cone conformation. The values of the dihedral angles between the phenolic rings and the plane R are respectively 77.15º, 32.68º, 65.91º and 44.37º. The dihedral angles between the opposing phenolic rings are 36.96º and 102.97º, respectively.

Within the asymmetric unit, two molecules of **8** form a host-to-host dimer (Fig. 4A). The π···π interactions between the parallel aromatic ring C of the dimer with aromatic centroid distance of 4.047Å, also support a weak C-H···π interaction with symmetry unique C(29)-H(29)···aromatic centroid distances of 3.072 Å. It is worth noting that the second fomyl group is introduced to the aromatic ring D (compared with **7·CHCl$_3$**), which gives rise to two weaker C-H···O interactions with symmetry unique C(6)-H(6)···O(5) and C(7)-H(7)···O(5) distances of 2.52 Å and 2.58 Å.

Cite this: DOI: 10.1039/c0xx00000x

www.rsc.org/xxxxxx

ARTICLE TYPE

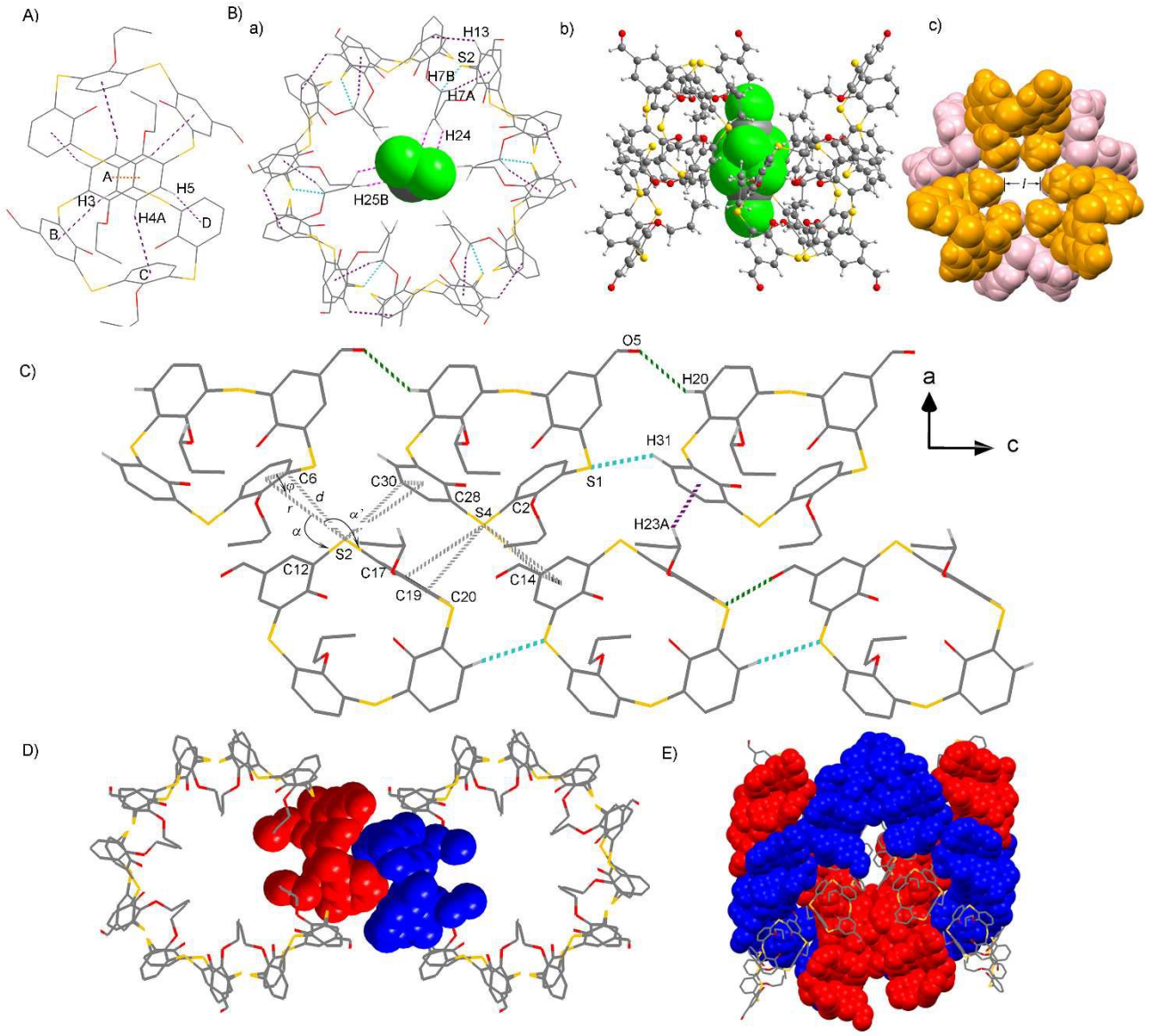

Fig. 3 (A) Host-to-host dimer assembly of **7·CHCl$_3$**. π···π and C-H···π interactions shown as orange and violet dotted lines, respectively. Hydrogen atoms (except for those involved in hydrogen bonding) are omitted for clarity. (B) Structure of **7·CHCl$_3$** showing hexameric discs, $CHCl_3$ resides the centre of the hexameric discs. a) View along the crystallographic *c* axis, C-H···π, C-H···S, and C-H···Cl interactions shown as violet, aqua and pink dashed lines, respectively. b) View along the crystallographic *a* axis (disordered $CHCl_3$ shown in two position). c) Space-filled representation of the hexameric disc structure of **1·CHCl$_3$ s**hown in alternating colour view along the crystallographic *c* axis. (C) View along the crystallographic *b* axis, stick diagram showing C-H···O, C-H···S, C-H···π, and S···π interactions are green, aqua, violet and gray dot lines in the crystal structure of **7·CHCl$_3$**. (D) Two hexameric disc 'emmeshed' by dimeric association of two thiacalixarene molecular, which coloured in blue and red. (E) Mixed space filling and stick representation side views of neighbouring nanotube in **7·CHCl$_3$**. $CHCl_3$ are omitted for clarity in the red and blue space filling.

Examination of the extended structure, the asymmetric unit forms a triply helical tube *via* several intermolecular interactions (Fig. 4B, Fig. S2 and S4). Within this arrangement, there is a weak C-H···O and a weak C-H···π interactions with C(29)-H(29)···O(2) and C(30)-H(30B)···aromatic centroid distances of 2.87 Å, and 2.66 Å, respectively. Two sets of S···π interactions (type III) with distances (*r*) and angels (*φ*) are in the range of 4.174-4.495 Å and 47.79-58.16º and other detail parameters are listed in Table S3.

Neighbouring tubes intermesh each other to form the 'honeycomb' architecture stabilised by non-covalent interactions (Fig. 4C and 4D). There are also three C-H···O interactions with

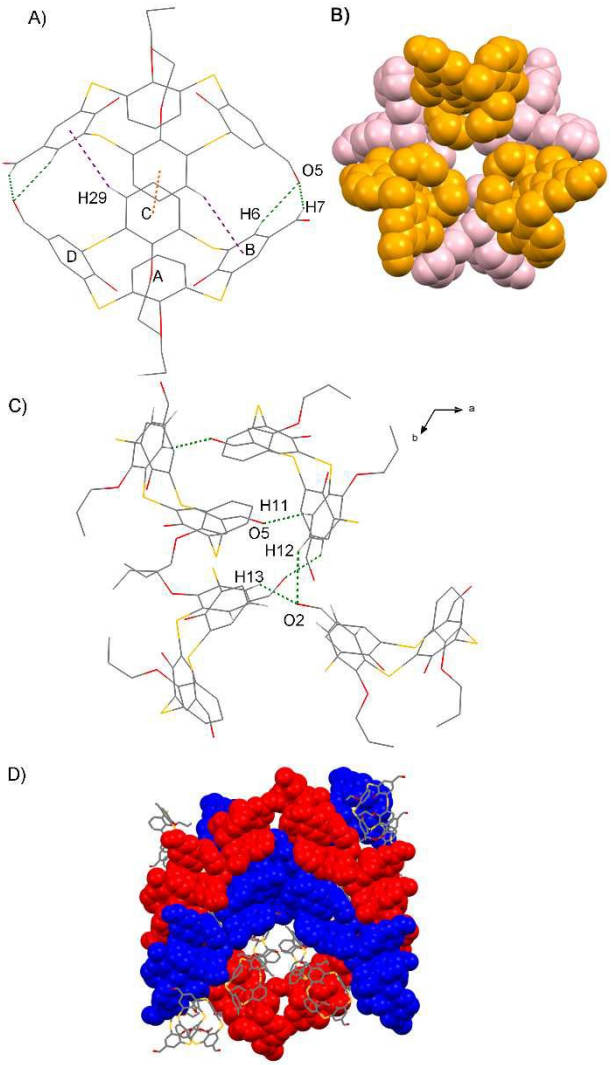

Fig. 4 (A) Host-to-host dimer assembly observed in the single crystal structure of **8**. C-H···π, π···π interactions shown as violet and orange dashed lines, respectively. (B) Space-filled representation of the hexameric disc structure of **8 s**hown in alternating colour. (C) C-H···O interactions observed in neighbouring nanotubes of **8**. C-H···O interactions shown as dashed green lines. (D) Mixed space filling and stick representation side views of neighbouring nanotube in **8**.

C(11)-H(11)···O(5), C(12)-H(12)···O(2) and C(13)-H(13)···O(2) distances of 2.39 Å, 2.59 Å and 2.46 Å, respectively. The inter-tubule distance is 21.52 Å and a complete cycle contains six thiacalix[4]arene molecules with distance of 36.76 Å (Table 1).

Crystal structure of 9

Guest-free crystals of **9** were obtained as colourless block crystals in the trigonal space group $R\bar{3}$, which are stabilised in a cone conformation. Formyl groups are highly disordered and it is difficult to determine the third formyl group's clear position of the crystals. According to the third formyl group's possible position, we denote compound **9** as **9a** and **9b**, respectively (Fig 5A), **9a** is modelled at 75% with refined site occupation factors. The values of the dihedral angles between the phenolic rings and the plane R are respectively 75.11º, 43.26º, 69.95º and 38.63º. The dihedral angles between the opposing phenolic rings are

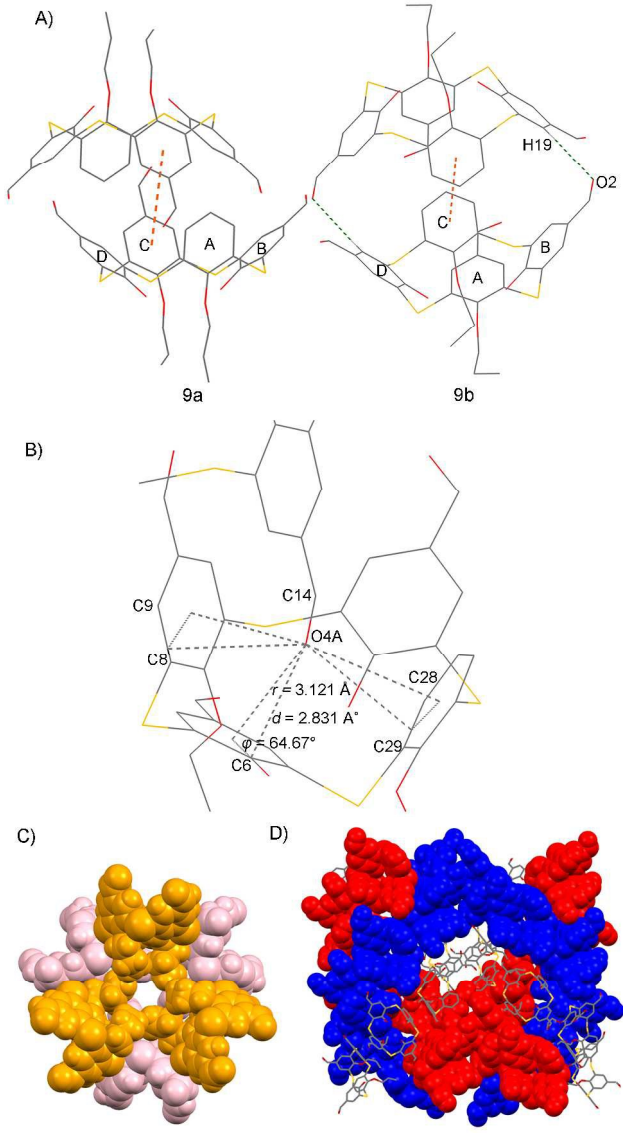

Fig. 5 (A) Host-to-host dimer assembly observed in the single crystal structure of **9a** and **9b**. (B) The O···π interactions observed in the dimer of **9a.** (C) Space-filled representation of the hexameric disc structure of **9a s**hown in alternating colour. (D) Mixed space filling and stick representation side views of neighbouring nanotube in **9a**.

34.97º and 98.10º. Compared with compound **8,** the third formyl group is introduced resulting in the dihedral angles of plane BD decrease nearly 7º.

Symmetry expansion of **9** reveals a novel host-to-host dimer motif. There is a weak π···π stacking with the aromatic centroid distance of 4.708 Å, which can be considered as being long interaction. In the dimer of **9a**, one formyl group of each molecule is located in the cavity of the other molecule forming C=O···π interactions[13c] between formyl group and aromatic rings (Fig. 5A). To our knowledge, this is the first time of observation of C=O···π interaction in the head-to-head dimer. The *r* distance from O(4A) to the aromatic ring B is 3.121 Å, while the *d* distance with C(14)=O(4A)···C(6) distance of 2.821 Å. corresponds to a 12.4% decrease in the sum of van der Waals radii[13c, 13e] (3.22 Å, Table S16). The C=O···π angles (α) is 155.7º, while the O···π-edge angle (φ) is 64.67° (Fig 5B). Other

Cite this: DOI: 10.1039/c0xx00000x

www.rsc.org/xxxxxx

ARTICLE TYPE

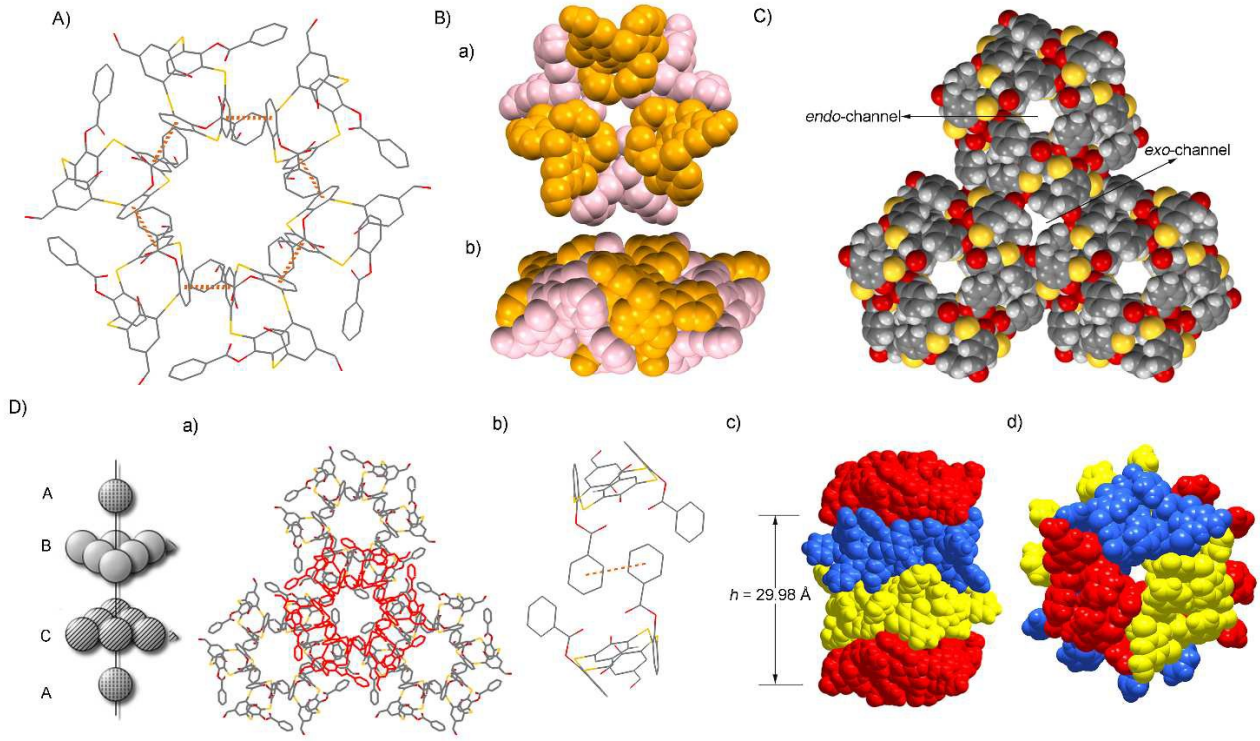

Fig. 6 (A) Structure of **10·H$_2$O** showing hexameric discs through π···π interactions as dashed orange lines. (B) Space-filled representation of the hexameric disc structure of **10·H$_2$O** shown in alternating colour. a) View along the crystallographic *c* axis and b) View along the crystallographic *a* axis. (C) In the 2D network, three hexameric rings are depicted in the CPK metaphor, which gives rise to the *exo*-channel and *the endo*-channel between adjacent hexameric discs. (D) Schematic of ccp packing of **10·H$_2$O**. a) Schematic of adjacent layers accumulate in the crystal structure of **10·H$_2$O**; b) Tail-to-tail dimer assembly observed in the single crystal structure of **10·H$_2$O**. π···π interactions shown as orange dashed lines; c) Side view showing stacked manner ABCABC···of **10·H$_2$O** coloured blue, yellow and red; d) Novel nanotubes of **10·H$_2$O** formed by ccp packing.

two sets of analogous C=O···π interactions the distances (*r*) all fall within acceptable range of 3.24 Å-3.558 Å (Tab. S6). In the case of **9b**, there is a weak C-H···O interaction with symmetry unique C(19)-H(19)···O(2) distance of 2.54 Å.

The asymmetric unit also forms a triply helical tube in an analogous fashion to aforementioned examples (Fig. S2 and Fig. 5C). View along the crystallographic *b* axis, this reveals the presence of two weaker C-H···π interactions with C(15')-H(15B)···aromatic centroid and C(32')-H(32A)···aromatic centroid respective distances of 2.96 Å and 2.92 Å in the case of **9a**, as compared to **9b**: C(15)-H(15C)···aromatic centroid and C(32)-H(32C)···aromatic centroid respective distances of 2.90 Å and 2.96 Å. A C-H···O interaction with C(11)-H(11)···O(2') distances of 2.61 Å in the case of **9a**, as compared to **9b**: C(26)-H(26)···O(2) distance of 2.99 Å (Fig. S5A). There are two sets of S···π interactions (type III) with distances (*r*) and angels (*φ*) ranging from 4.149 Å to 4.252 Å and 55.43º to 63.31º, and other detail metric parameters are given in Table S3.

Neighbouring tubes intermeshing each other also form the 'honeycomb' architecture stabilised by non-covalent interactions (Fig. S2 and 5D). In the case of **9b**, there are two C-H···O interactions with C(26)-H(26)···O(4B) and C(28)-H(28)···O(2) distances of 2.09 Å and 2.49 Å, respectively (Fig. S5B). The inter-tubule distance is 22.01 Å and a complete cycle with a repeat distance of 35.76 Å (Table 1).

Crystal structure of 10·H$_2$O

10·H$_2$O and **11** were reported by our previously text,[23] but we haven't discussed their self-assembly of supramolecular structure. Single crystals of **10·H$_2$O** are in a trigonal cell, and structure was performed in the space group $R\bar{3}$. The asymmetric unit consists of one molecule of **10** and one H$_2$O molecule. Compound **10** also adopts a cone conformation in the solid state. Introduction of formyl groups to the upper rim results in the geometries that have remarkable changes in the solid state (Fig. S6A). The rings A and C are flipped inward toward each other in a face-to-face fashion, almost blocking the molecular cavity, whereas the remaining rings B and D are flipped outward. The values of the dihedral angles between the phenolic rings and the reference molecular plane R are equal to 110.16º, 20.73º, 109.25º and 28.42º, respectively. The dihedral angles between the opposing phenolic rings are 39.42º and 130.59º. The classical head-to-head dimer is no longer present. In the 2D network, view along the crystallographic *c* axis, six molecules of compound **10** form the

Cite this: DOI: 10.1039/c0xx00000x

www.rsc.org/xxxxxx

ARTICLE TYPE

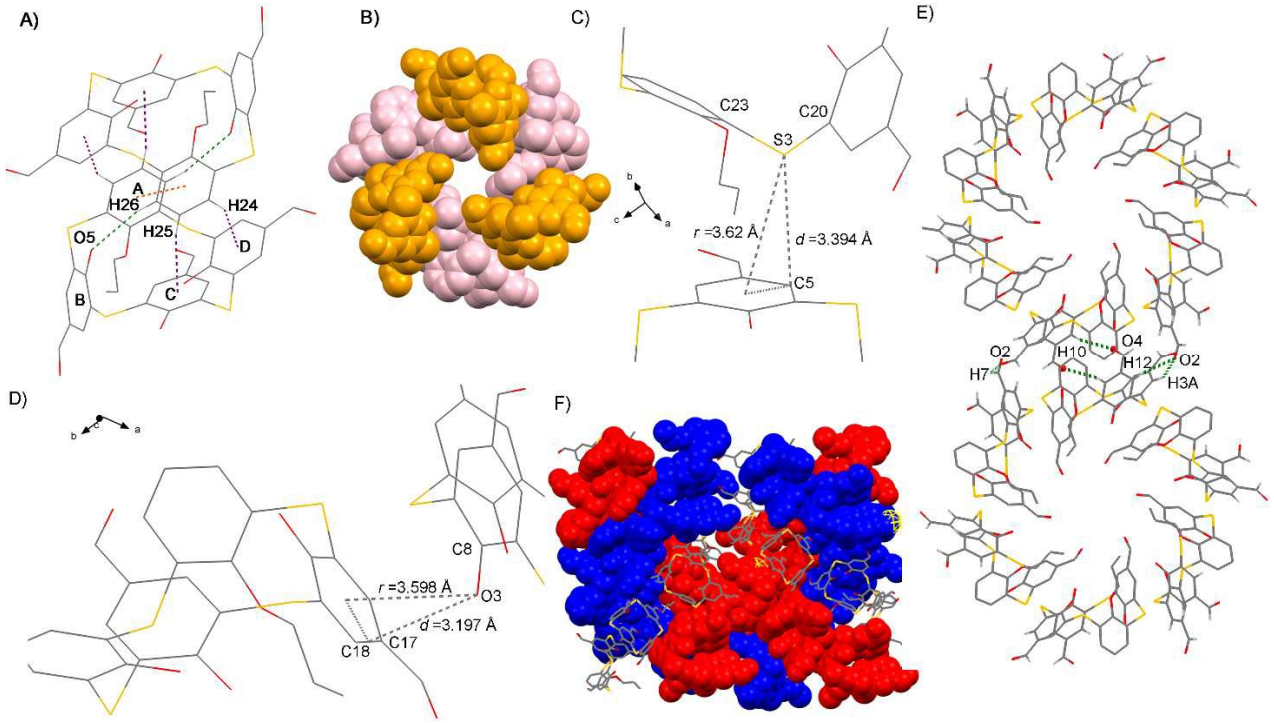

Fig. 7 (A) Head-to-head dimer assembly observed in the single crystal structure of **11**. (B) Space-filled representation of the hexameric disc structure of **11** shown in alternating colour. (C) The S···π interactions observed in hexameric discs formed by crystallisation of **11**. (D) O···π interactions observed in hexameric discs formed by crystallisation of **11**. (E) The C-H···O interactions observed in the neighbouring hexameric disc, which form 'cylindrical helical gear' fashion. (E) Mixed space filling and stick representation side views of neighbouring nanotube in **11**.

hexameric disc *via* π···π stacking with aromatic centroid distances of 3.725 Å (Fig. 6A and Fig. S6B), which is supported by two sets of S···π interactions and the distances (*r*) all fall within acceptable range of 4.082-4.106 Å. Each individual hexameric almost in the same plane is linked to neighbouring hexameric through S···π, C=O···π and C-H···π interactions form a 'Ferris wheels' shape (Fig. 6B, 6C and Fig. S6C).[4a, h] The S(1)···π interactions (Type II) with distances (*r*) and angels (*φ*) are 4.753 Å and 38.51º, which can be considered as long S···π interactions. The C(40)=O(8)···π interactions with distances (*r*) and angels (*φ*) are 3.832 Å and 60.91º. The C-H···π interaction with symmetry unique C(38)-H(38)···aromatic centroid distance of 3.113 Å.

Unlike the previous structures, the crystal lattice reveals a novel tubular superstructure. Each hexameric disc as the basic unit, the 'Ferris wheels' architecture layers further accumulate in a cubic closest packed manner (ccp) into a 3D network (Fig 6D). In addition, two molecules of **10** to form a tail-to-tail dimer *via* π···π stacking between the lower rim substituted of aromatic ring of adjacent layers hexameric disc with aromatic centroid distance of 4.801 Å. (Fig 6D(b)). In addition, two sets of S···π interactions all fall within acceptable range of 4.254-4.891 Å and a weaker C-H···O interaction with symmetry unique C(36)-H(36)···O(8) distance of 2.735 Å (Fig. S6D and S6E). These basic units are aligned parallel but off-centred and shifted 22.31 Å (Fig. S6D) from the previous hexameric disc of perpendicular as measured by the channel axis. Close inspection of the extended structure reveals that the nanotubes can be viewed together constituting the *endo*- channel (hollow spaces of hexameric discs) and the *exo*-channel (the interstitial space between the neighbouring hexameric discs) (Fig. 6D). It is worth noting that water molecules within these channel.

The greater bulk of benzoyl groups is introduced to the lower rim, but more compacts pack in the molecule. A complete cycle contains ABCABC···stack with a repeat distance of 29.98 Å (compares with **8**, 36.76 Å) and the distance between the nanotubes is 22.31 Å (Table 1).

Crystal structure of 11

Single crystals of **11** are in a trigonal cell, and structure was performed in the space group $R\bar{3}$. The asymmetric unit is composed of one thiacalix[4]arene molecule which adopts a *partial-cone* conformation, with no observed solvent incorporation. The formyl group of phenolic ring B is small enough to allow rotation of aromatic ring *via* 'the lower rim through annulus' pathway.[5b, 15c] Phenolic ring C and phenolic ring D are highly disordered over two positions, and the non-disordered situation is modelled at 70.7% with refined site

Cite this: DOI: 10.1039/c0xx00000x

www.rsc.org/xxxxxx

ARTICLE TYPE

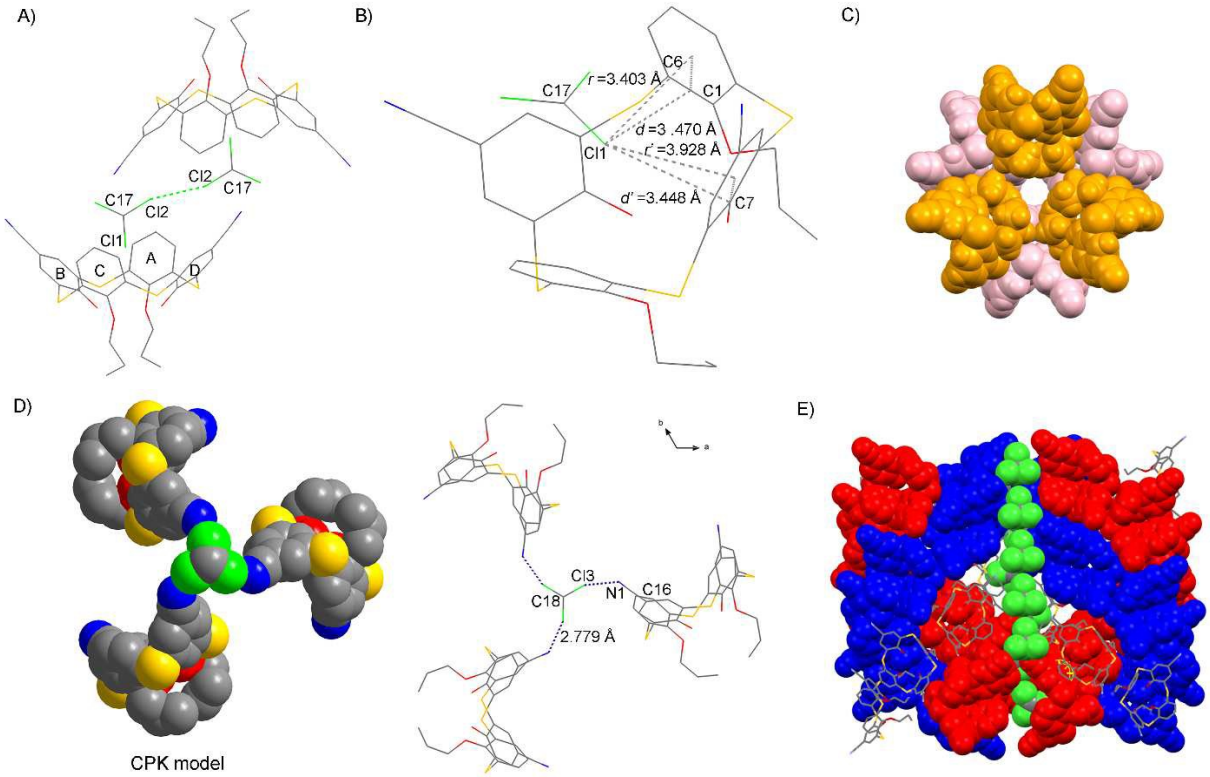

Fig. 8 (A) $CHCl_3$ templated dimerisation of **12·CHCl$_3$**. Cl···Cl interactions shown as dashed bright green lines. (B) The Cl···π interactions observed in the dimer. (C) Space-filled representation of the hexameric disc structure of **12** shown in alternating colour. (D) The C-N···Cl interaction found in the packing between neighbouring hexameric discs of **12·CHCl$_3$**. (E) Mixed space filling and stick representation side views of neighbouring nanotube in **12·CHCl$_3$.**

occupation factors. The values of the dihedral angles between the aromatic rings and the reference molecular plane R are respectively 78.60º, 89.92º, 73.46º and 43.25º. The dihedral angles between the opposing aromatic rings are 27.98º and 46.84º, respectively.

Within the asymmetric unit, two molecules of **11** form a head-to-head dimer via π···π stacking between the parallel aromatic ring A with aromatic centroid distance of 4.300 Å (Fig. 7A). Compared with compound **9**, the distance of the parallel aromatic ring A has shorten 0.4 Å, which might be related to the fact that the inverted aromatic ring B reduces the repulsion between the dimer. By the inversion, OH groups give rise to two weaker CH···O interactions with symmetry unique C(26)-H(26)···O(5) distance of 2.73 Å. In addition, there are also two C-H···π interactions between with symmetry unique C(24)-H(24)···aromatic centroid and C(25)-H(25)···aromatic centroid distances of 2.65 Å and 2.90 Å, respectively.

The back-to-back packing arrangement forms a triply helical tube which is directed by S···π, C-O···π and C-H···O interactions (Fig. 7B, 7C, 7D, Fig. S2 and S7). In this case, the S(3)···π interactions can be classified as Type I.[13e] The distances from S(3) to the aromatic rings centre (r) is 3.620 Å, and the value is 0.82% shorter than the sum of van der Waals radii, while the closest aromatic ring edge (d) is 3.394 Å. The angel of C(20)–S(3)···centroid (α), C(23)-S(3)···centroid (α') and angel φ are 104.0º, 129.52º and 69.57º, respectively. There are other two sets of S···π interactions (type II) with distances (r) and angels (φ) in range of 3.979-4.260 Å and 42.87-60.77º, respectively. Other detail parameters are shown in Table S3. As is shown in Fig. 7D, a C-O···π interaction between the phenolic oxygen atom located directly opposite to the inverted aromatic ring B with C(8)-O(3)···aromatic centroid (r) is 3.598 Å, while the closest aromatic ring edge (d) is 3.189 Å. The C(8)-O(3)···centroid (α) and O(3)···centroid-edge angles (φ) are 84.55° and 60.93°. There is presence of two weaker C-H···O interactions with C(5)-H(5)···O(4) and C(29)-H(29A)···O(6) distances of 2.82 Å and 2.54 Å, respectively.

Neighbouring hexameric link to each other to form as 'cylindrical helical gear' fashion nanotube, which is stabilised by C-H···O interactions with C(3)-H(3A)···O(2), C(7)-H(7)···O(2), C(10)-H(10)···O(4) and C(12)-H(12)···O(2) distances of 2.53 Å, 2.53 Å, 2.63 Å and 2.75Å, respectively (Fig. 7E and 7F). The inter-tubule distance is 21.99 Å and a complete cycle repeat with a distance of 32.04 Å (Table 1).

Cite this: DOI: 10.1039/c0xx00000x

www.rsc.org/xxxxxx

ARTICLE TYPE

Table 1

Compound	β/° (Plane BD) [a]	*r*/Å (In the range of S···π interactions) [a]	*D*/Å (π···π interactions in dimer)	*l*/Å (The inner diameter of the nanotube) [a]	*L*/Å (The distance between neighbouring nanotube) [a]	*h*/Å (The distance with a repeat cycle) [a]
2	113.72	4.104 - 4.250	3.886(5)	7.88	20.94	35.72
7·CHCl$_3$	109.6	4.127 - 4.357	4.050(3)	7.67	21.34	35.45
8	102.97	4.174 - 4.495	4.047(2)	5.93	21.19	36.76
9	98.10	4.149 - 4.252	4.708(3)	5.33	22.01	35.76
10·H$_2$O	-	4.082 - 4.891	3.725(3)	8.53	22.31	29.98
11	-	3.625 - 4.260	4.300(4)	7.06	21.99	32.04
12·CHCl$_3$	92.06	3.946 - 4.215	-	6.01	23.99	34.94

[a] Measure by MERCURY

Crystal structure of 12·CHCl$_3$

The crystals of **12·CHCl$_3$** were obtained as colourless needle crystals in the trigonal space group $P\bar{3}\,c1$ with the asymmetric unit is composed of a half of thiacalix[4]arene molecule lying about a two-fold axis, a half of chloroform molecules lying about a two-fold axis and one-third chloroform molecules lying about a three-fold axis. In the solid state, compound **12** adopts a cone conformation with C_2 symmetry. The values of the dihedral angles between the phenolic rings and the plane R are equal to 68.73º and 43.97º. The dihedral angles between the opposing phenolic rings are 42.54º and 92.06º.

In comparison to compound **8**, the formyl groups are replaceable by the cyano groups make dramatic changes in crystal structure. Within the asymmetric unit, Cl···Cl and Cl···π interactions form a unique off-set[3b] arrangement of the dimer. In the dimer, adjacent thiacalix[4]arene molecular are linked through $CHCl_3$. One chlorine atom of the chloroform is lodged in the π-basic host cavity, while the other chlorine atoms form Cl···Cl contacts of the dimerisation shown in Fig. 8A and 8B. In this case, the Cl···Cl interactions can be classified as Type I[12d] (Fig.S8) The Cl···Cl interaction with C(17)-Cl(2)···Cl(2)-C(17) distance is 2.921 Å, θ_1 and θ_2 angle are 151.43° in the dimer. Similar to the S···π interactions, the Cl···π interactions[13c] distance is defined as *r*, while *d* represents the distance from the Cl atom to the closest ring atom, the angle between the Cl···centroid axis and the ring plane is denoted by φ, and the C-Cl···centroid angle is represented by α in the present context. The *r* distance from Cl(1) to the aromatic ring A is 3.403 Å, while the *d* distance from Cl(1) to the corresponding ring edge (between C(1) and C(6) is 3.470Å. The C(17)-Cl(1)···π angles (α) is 104.52º, while the Cl···π-edge angle (φ) is 83.20°. The *r'* distance from Cl(1) to the aromatic ring B is 3.928 Å, while the *d'* distance from Cl(1) to the nearest carbon atom C(7) is 3.448 Å. The angle (α') is 106.87º and the Cl···π-edge angle (φ') is 60.14°.

The asymmetric unit also forms a triply helical tube *via* S···π and C-H···π interactions (Fig. S2, S9A and Fig.7C). Two sets of S···π interactions with *r* and φ are in the range of 3.946 Å-4.215 Å and 62.38º-62.95º, respectively. The C-H···π interactions with C(13)-H(13B)···aromatic centroid distances of 2.84 Å (Fig. S9B).

Symmetry expansion of the crystal structure of **12·CHCl$_3$** reveals that a trimeric unit is held together by stronger C-N···Cl interactions (Fig. 8D). The trimeric unit has a C_3 symmetry axis with the host molecules located around it. The cyano···halogen interactions with C(16)-N(1)···Cl(3) distance is 2.779 Å, which is 15.8% shorter than the sum of van der Waals radii (3.3 Å, Table S16), while the C(16)–N(1)···Cl(3) and C(18)-Cl(3)···N(1) angles are 147.94°and 149.85°, respectively. The off-set dimeric and trimeric unit act as bridges between neighbouring nanotubes, while the *exo*-nanotube is filled with chloroform molecules (Fig. 2 and 8E). The distance between the nanotubes is 23.99 Å and a complete triple helix repeat distance is 34.94 Å (Table 1).

Discussion

Partially-O-substituted at the lower rim, and then upper-rim changed, the six thiacalix[4]arene molecules that pack in a back-to-back fashion form hexameric disc and 'honeycomb' architecture nanotube.

Examination of the structure of **7·CHCl$_3$**, **8** and **9** shows that the thiacalixarene has larger cavities and more favours of interdigitation aromatic yielding the head-to-head dimeric motif via π···π interactions. With the number of aldehyde groups increasing, the dihedral angles of plane BD (β) gradually decreases, the distance between parallel aromatic rings of the dimer (*D*) more and more far away. The distance (*D*) is increasing from 4.050 to 4.708Å (Table 1). We speculate that this is due to the steric crowding of neighbouring upper rim formyl groups. Taking into account the results obtained with compound **9** and **11**, the invert aromatic ring B of **11** reduces the repulsion of parallel aromatic ring between the head-to-head dimer and gives rise to strong S···π interaction (*r*=3.620 Å) slightly below the van der Waals contacts. It is conducive to the formation of hexameric disc. Although molecule **10** is stabilised in its cone conformation, the head-to-head dimeric structure breaks down due to the introduction of the greater bulk of benzoyl groups. The lower rim benzoyl groups form the tail-to-tail dimer *via* π···π interactions and are both positioned on the *endo*- and *exo*-hexameric disc while other five compounds assembles the lower rim groups which are found at the *endo*-hexameric disc. From these we realised that the dimer motif via π···π interactions is almost omnipresent in the thiacalixarene.

The formation of 'honeycomb' nanotubes is strongly dependent on dimerisation of each host molecules through complement π···π interactions. When π···π interactions are absent, solvent may help host molecule to form the architectures. In compound **12**, the dihedral angles of plane BD (*β*) decreases to 92.09°, making neighbouring **12** cannot connect to each other by π···π interactions and the distance between neighbouring nanotubes *(L*=23.99 Å) is longer than other five compounds (*L*=21.19-22.31 Å). Instead, they are linked together through the connection of solvent molecules. $CHCl_3$ molecules are oriented so as to form Cl···Cl, Cl···π and cyano···Cl interaction with neighbouring nanotubes.

S···π interaction can work in a positive way, making the molecules assembling tightly stacked. The distance of S···aromatic rings centre (*r*) and the distance with a repeat cycle (*h*), to a certain extent, reflect the stability of the crystal. The shorter the distance of S···aromatic rings centre (*r*) is, the smaller the distance with a repeat cycle (*h*) is, resulting in the molecules more tightly stacked and crystals even more stable (Table 1). Compared with compound **8,** the distance with a repeat cycle (*h*) of **10·H_2O** has decreased approximately 6 Å, which implies more compact pack in the **10·H_2O** molecule. Compared with compound **9,** the distance with a repeat cycle (*h*) of compound **11** has decreased from 35.76 to 32.04 Å, which also implies more tightly stacked and more stable in compound **11**. From these we realised that the variation in the conformation of the host molecules does not dominate the hexameric disc formation in this case. As long as host molecules can be circumvented in an appropriate manner to form disk-shaped hexameric with S···π interactions.

The inner diameter of the nanotube (*l*) of **12** (6.01 Å) is equal to **9** (5.93 Å) with a reasonable deviation, which implies that molecules aggregates form a closed disk-shaped hexameric, is driven by the presence of lower rim propoxy when host molecule adopts similar cone conformation. From **7·$CHCl_3$** to **9**, with the number of aldehyde groups increasing, the inner diameter of the nanotube (*l*) is shrinking from 7.67 to 5.33Å. Different numbers of aldehyde at upper-rim have an effect on the crystal packing and the propoxy groups are closer towards the centre of the tubes. These thiacalix[4]arene molecules have some flexibility and the inner diameter of nanotube (*l*) is in the range of 5.33-8.53 Å, which may act as storage or as a transport channel for small molecules,[5h] such as helium, hydrogen, chloroform or water.

Conclusion

We have demonstrated that modest changes in the primary structure of thiacalix[4]arene can build 'honeycomb' structure through a set of weak interactions and shape complementarity, indicating the great stability of the non-covalent organic framework. Despite the variation in the conformation of host molecules, there is little difference in the solid with nearly the same unit cell dimensions and space group symmetry. The host scaffolds and solvent play a crucial role in supramolecular arrays. S···π, O···π and π···π interactions tend to associate into their characteristic nanotube. Knowledge of this behaviour will serve as further insights in controlling the assembly of hollow tubular architectures in the solid state.

Experimental

Compound **7**. According to the literature,[17b, 23] compound **5** was allowed to react for 2 days to give **7** after purification ($CHCl_3$) as a white solid. Conversion: 4%.

^{1}H NMR (300 MHz, $CDCl_3$) δ 9.88 (s, 1 H, CHO), 8.33 (s, 1 H, ArOH), 8.18 (s, 2 H, ArH), 7.63 (d, *J* = 7.5 Hz, 2 H, ArH), 6.96 (t, *J* = 8.7 Hz, 4 H, ArH), 6.81 (t, *J* = 5.2 Hz, 1 H, ArH), 6.58 (t, *J* = 7.9 Hz, 2 H, ArH), 4.32 (s, 4 H, $ArOCH_2$), 2.04 (d, *J* = 6.8 Hz, 4H), 1.17 (t, *J* = 7.5 Hz, 6H) ppm. ESI-MS: *m/z* = 631 $[M+Na]^+$.

Compound **12**. According to the literature,[17c] compound **8** (0.1g, 0.157mmol) and NH_2OH (15.7mmol) in water were added to acetonitrile (15 mL), and the mixture was heated to reflux for **12** to the mixture extracted with dichloromethane. The organic layer was washed with water and dried with $MgSO_4$. The solution was filtered and the solvent removed under reduced pressure. The residue was purified by using column chromatography with 1:1 hexane/dichloromethane to give 10 (35mg, 35%) as a white solid.

^{1}H NMR (300 MHz, $CDCl_3$): δ 8.43 (s, 2 H, ArOH), 7.87 (s, 4H, ArH), 7.05 (d, *J* = 7.8 Hz, 4 H, ArH), 6.65 (t, *J* = 7.7 Hz, 4 H, ArH), 4.21 (t, *J* = 6.6 Hz, 4 H, $ArOCH_2$), 1.99 (m, 4 H, CH_2), 1.12 (t, *J* = 7.4 Hz, 6 H, CH_3) ppm. ESI-MS: *m/z* = 629 $[M-H]^-$.

X-Ray crystallography

X-Ray data of the crystals were collected on a 'Bruker SMART CCD' or 'APEX-II CCD' single-crystal diffractometre with graphite filtered Mo-Ka (λ= 0.71073 Å) radiation. Data collections for crystals of **7·$CHCl_3$** and **11** were carried out at 100(2) K. For **8** was carried out at 173(2) K. For **9, 10·H_2O** and **12·$CHCl_3$** were carried out at room temperature. The structures was solved by direct methods. **7·$CHCl_3$**, **8** and **9** refined by Fullmatrix least-squares on F^2 using SHELXS-97[24], **10·H_2O** refined by Fullmatrix least-squares on F^2 using SHELXS-2014, **5** and **10·$CHCl_3$** refined by Fullmatrix least-squares on F^2 using SHELXS-2013. Diagrams and publication material were generated using WinGX,[25] and PLATON. All the non-hydrogen atoms were located directly by successive Fourier calculations and were refined anisotropically. Hydrogen atoms except for that of the disordered lattice solvent molecule and water molecule were placed in geometrically calculated positions by using a riding model.

Referring to compound **7·$CHCl_3$**, one phenolic ring and $CHCl_3$ molecules were found to be disordered. C(26)–C(32), S(3) and O(4) were refined with a split atom model. The occupancy factors are 0.859 for C(26)–C(31), S(3) and O(4), 0.141 for C(26')–C(31'), S(3') and O(4') , C(32) for 0.5 at two positions, Cl atoms are severely disordered which could not be modelled by discrete atoms in the compound. (Table S17). Commands 'DFIX' and 'SADI' were used in the above refinement.

In compound **8**, one propoxy group was found to be disordered. Split atoms were used for C(14), C(15) and C(16). The occupancy factors are 0.826 for C(14)-C(16), 0.174 for C(14')-C(16'). Commands 'DFIX', 'MISU' and 'SADI' were used in the above refinement.

In compound **9**, three formyl groups and two propoxy groups were found to be disordered. Split atoms were used for C(14)-C(17), C(32)-C(34), O(4), O(2) and O(6). The occupancy factors are 0.75 for C(14), 0.57 for C(15)–C(17), 0.66 for C(32)-C(34),

0.69 for O(2) and 0.78 for O(6), 0.25 for C(14B), 0.43 for C(15')–C(17'), 0.34 for C(32')-C(34'), 0.31 for O(2') and 0.22 for O(6'). O(4), O(4A) and O(4B) atoms were disordered over three positions. Two reside around the C(14) atoms and the third one reside around the C(14B) atom. The occupancy factors are 0.375 for O(4), 0.375 for O(4A) and 0.25 for O(4B). Commands 'DFIX' and 'FLAT' were used in the above refinement.

Commands 'DELU' and 'ISOR' were used in the refinement of compound **10·H_2O.**

In compound **11**, one propoxy group and two phenolic ring were found to be disordered. Split atoms were used for C(15)-C(30), S(2), S(3), S(4), O(5), O(6) and O(7). The occupancy factors are 0.707 for C(15)-C(30), S(2)-S(4) and O(5)-O(7), 0.293 for C(15')-C(30'), S(2')-S(4') and O(5')-O(7'). Commands 'EADP', 'ISOR', 'SIMU' and 'FLAT' were used in the above refinement.

The crystals of **12·$CHCl_3$** were very weakly diffracting, although several data collections of the same material were performed on these single crystals, and no improvement was observed. The solvent molecules are the most likely reason for poor diffraction and subsequent abnormally high R-factors associated with these crystals. Two $CHCl_3$ were found to be disordered. Split atoms were used for Cl(2) and Cl(3). The occupancy factors are 0.6 for Cl(2), 0.75 for Cl (3), 0.4 for Cl(2') and 0.75 for Cl (3'). Commands 'SIMU', 'ISOR' and 'DFIX' were used in the above refinement.

Acknowledgements

We are grateful to the National Natural Science Foundation of China (20772092) and the Hubei Province Natural Science Fund for Distinguished Young Scholars (2007ABB021) for financial support.

Notes and references

[a] *College of Chemistry and Molecular Sciences, Wuhan University, Wuhan 430072, PR China*

[b] *Key Laboratory of Tobacco Flavor Basic Research, Zhengzhou Tobacco Research Institute of CNTC, No. 2, Fengyang Street, High-Tech Zone, 450001 Zhengzhou, China*

* *Corresponding Author: E-mail: gongsl@whu.edu.cn; Fax: +86 27 68754067; Tel: +86 27 68752701.*

†Electronic Supplementary Information (ESI) available: spectral characterisation data (^{1}HNMR, ESI-MS), supporting figure and supporting table, Crystallographic information file (cif). CCDC reference numbers 867095, 867096, 1056803-1056806. For ESI and crystallographic data in CIF or other electronic format see DOI: 10.1039/c0xx00000x

1. J. Sánchez-Quesada, M. P. Isler and M. R. Ghadiri, *Journal of the American Chemical Society*, 2002, 124, 10004-10005.
2. (a) G. Kerric, E. J. Parra, G. A. Crespo, F. Xavier Rius and P. Blondeau, *Journal of Materials Chemistry*, 2012, 22, 16611-16617; (b) Y. Wen, T. Sheng, Z. Xue, Y. Wang, C. Zhuo, X. Zhu, S. Hu and X. Wu, *Inorganic chemistry*, 2015, 54, 3951-3957.
3. (a) O. V. Kulikov, M. M. Daschbach, C. R. Yamnitz, N. Rath and G. W. Gokel, *Chemical Communications*, 2009, 7497-7499; (b) A. K. Maerz, D. A. Fowler, A. V. Mossine, M. Mistry, H. Kumari, C. L. Barnes, C. A. Deakyne and J. L. Atwood, *New Journal of Chemistry*, 2011, 35, 784-787.
4. H. Mansikkamaki, M. Nissinen and K. Rissanen, *Angewandte Chemie*, 2004, 43, 1243-1246.
5. (a) G. W. Orr, *Science*, 1999, 285, 1049-1052; (b) A. W. Coleman, E. Da Silva, F. Nouar, M. Nierlich and A. Navaza, *Chem Commun (Camb)*, 2003, 826-827; (c) G. G. S. L. G. Kuz'mina, J. A. K. Howard, É. A. Shokova, and V. V. Kovalev, *Crystallography Reports,*, 2003, 48, 267; (d) S. J. Dalgarno, J. L. Atwood and C. L. Raston, *Chem Commun (Camb)*, 2006, 4567-4574; (e) A. N. Lazar, N. Dupont, A. Navaza and A. W. Coleman, *Chem Commun (Camb)*, 2006, 1076-1078; (f) F. Perret, A. N. Lazar, O. Shkurenko, K. Suwinska, N. Dupont, A. Navaza and A. W. Coleman, *CrystEngComm*, 2006, 8, 890; (g) A. Lazar, O. Danylyuk, K. Suwinska, F. Perret and A. W. Coleman, *Chem Commun (Camb)*, 2006, 903-905; (h) S. J. Dalgarno, P. K. Thallapally, L. J. Barbour and J. L. Atwood, *Chemical Society reviews*, 2007, 36, 236-245; (i) S. J. Dalgarno, J. E. Warren, J. Antesberger, T. E. Glass and J. L. Atwood, *New Journal Of Chemistry*, 2007, 31, 1891-1894; (j) R. M. McKinlay and J. L. Atwood, *Angewandte Chemie International Edition*, 2007, 46, 2394-2397; (k) S. Kennedy and S. J. Dalgarno, *Chem Commun (Camb)*, 2009, 5275-5277; (l) S. Kennedy, G. Karotsis, C. M. Beavers, S. J. Teat, E. K. Brechin and S. J. Dalgarno, *Angewandte Chemie*, 2010, 49, 4205-4208; (m) S. Kennedy, S. J. Teat and S. J. Dalgarno, *Dalton transactions*, 2010, 39, 384-387; (n) S. Kennedy, C. M. Beavers, S. J. Teat and S. J. Dalgarno, *New Journal Of Chemistry*, 2011, 35, 28-31; (o) S. Kennedy, C. M. Beavers, S. J. Teat and S. J. Dalgarno, *Crystal Growth & Design*, 2012, 12, 679-687; (p) S. Kennedy, I. E. Dodgson, C. M. Beavers, S. J. Teat and S. J. Dalgarno, *Crystal Growth & Design*, 2012, 12, 688-697; (q) S. Kennedy, P. Cholewa, R. D. McIntosh and S. J. Dalgarno, *Crystengcomm*, 2013, 15, 1520-1523; (r) C.-X. Lin, X.-F. Kong, Q.-S. Li, Z.-Z. Zhang, Y.-F. Yuan and F.-B. Xu, *CrystEngComm*, 2013, 15, 6948-6962; (s) S. Kennedy, C. M. Beavers, S. J. Teat and S. J. Dalgarno, *CrystEngComm*, 2014, 16, 3712-3717; (t) G.-L. Zheng, G.-C. Yang, S.-Y. Song, X.-Z. Song and H.-J. Zhang, *CrystEngComm*, 2014, 16, 64-68; (u) X.-T. Li, J. Li, M. Li, Y.-Y. Liu, S.-Y. Song and J.-F. Ma, *CrystEngComm*, 2014, 16, 9520-9527.
6. G. R. Desiraju, *Nature*, 2001, 412, 397-400.
7. (a) M. C. Etter, *The Journal of Physical Chemistry*, 1991, 95, 4601-4610; (b) R. H. Vreekamp, W. Verboom and D. N. Reinhoudt, *J Org Chem*, 1996, 61, 4282-4288; (c) T.-F. Tan, J. Han, M.-L. Pang, H.-B. Song, Y.-X. Ma and J.-B. Meng, *Crystal Growth & Design*, 2006, 6, 1186-1193; (d) K. T. Holman, *Angewandte Chemie*, 2011, 50, 1228-1230.
8. (a) Z. S. Derewenda, L. Lee and U. Derewenda, *Journal of Molecular Biology*, 1995, 252, 248-262; (b) G. R. Desiraju, *Accounts of chemical research*, 1996, 29, 441-449; (c) Y. Gu, T. Kar and S. Scheiner, *Journal of the American Chemical Society*, 1999, 121, 9411-9422; (d) C. Janiak and T. G. Scharmann, *Polyhedron*, 2003, 22, 1123-1133; (e) R. Carrillo, M. Lopez-Rodriguez, V. S. Martin and T. Martin, *CrystEngComm*, 2010, 12, 3676-3683; (f) A. Shkurenko, H. Seriouna, K. Kedim, J.-B. Gervès, K. Suwinska and A. Coleman, *Journal of Chemical Crystallography*, 2014, 44, 380-385.
9. M. Domagala and S. J. Grabowski, *The Journal of Physical Chemistry A*, 2005, 109, 5683-5688.
10. (a) N. N. Laxmi Madhavi, G. R. Desiraju, A. K. Katz, H. L. Carrell and A. Nangia, *Chemical Communications*, 1997, 1953; (b) M. Nishio, M. Hirota and Y. Umezawa, 1998; (c) Y. Umezawa, S. Tsuboyama, K. Honda, J. Uzawa and M. Nishio, *Bulletin of the Chemical Society of Japan*, 1998, 71, 1207-1213; (d) Z. Zhang, Y. Luo, J. Chen, S. Dong, Y. Yu, Z. Ma and F. Huang, *Angewandte Chemie*, 2011, 50, 1397-1401; (e) C. Fischer, T. Gruber, D. Eissmann, W. Seichter and E. Weber, *Crystal Growth & Design*, 2011, 11, 1989-1994; (f) M. Nishio, Y. Umezawa, J. Fantini, M. S. Weiss and P. Chakrabarti, *Physical Chemistry Chemical Physics*, 2014, 16, 12648-12683.
11. (a) G. R. Desiraju and R. L. Harlow, *Journal of the American Chemical Society*, 1989, 111, 6757-6764; (b) A. Vargas Jentzsch, A. Hennig, J. Mareda and S. Matile, *Accounts of chemical research*, 2013, 46, 2791-2800.
12. (a) P. Metrangolo and G. Resnati, *Chem-Eur J*, 2001, 7, 2511-2519; (b) F. F. Awwadi, R. D. Willett, K. A. Peterson and B. Twamley, *Chem-Eur J*, 2006, 12, 8952-8960; (c) T. T. T. Bui, S. Dahaoui, C.

Lecomte, G. R. Desiraju and E. Espinosa, *Angewandte Chemie International Edition*, 2009, 48, 3838-3841; (d) M. Yamada and F. Hamada, *Crystal Growth & Design*, 2015, 15, 1889-1897.
13. (a) T. Korenaga, H. Tanaka, T. Ema and T. Sakai, *Journal of fluorine chemistry*, 2003, 122, 201-205; (b) R. Bishop, M. L. Scudder, D. C. Craig, A. N. M. Rahman* and S. F. Alshahateet*, *Molecular Crystals and Liquid Crystals*, 2005, 440, 173-186; (c) T. J. Mooibroek, P. Gamez and J. Reedijk, *CrystEngComm*, 2008, 10, 1501-1515; (d) H. Matter, M. Nazaré, S. Güssregen, D. W. Will, H. Schreuder, A. Bauer, M. Urmann, K. Ritter, M. Wagner and V. Wehner, *Angewandte Chemie*, 2009, 121, 2955-2960; (e) C.-Q. Wan, J. Han and T. C. Mak, *New Journal of Chemistry*, 2009, 33, 707-712; (f) X.-L. Gao, L.-P. Lu and M.-L. Zhu, *Acta Crystallographica Section C: Crystal Structure Communications*, 2009, 65, 123-127; (g) X. Pang, H. Wang, X. R. Zhao and W. J. Jin, *CrystEngComm*, 2013, 15, 2722-2730.
14. (a) T. Caronna, R. Liantonio, T. A. Logothetis, P. Metrangolo, T. Pilati and G. Resnati, *Journal of the American Chemical Society*, 2004, 126, 4500-4501; (b) B.-T. Zhao, H. Wang, H.-Y. Zhang and Y. Liu, *Journal of Molecular Structure*, 2005, 740, 101-105.
15. (a) J. L. Atwood, L. J. Barbour, M. J. Hardie and C. L. Raston, *Coordination Chemistry Reviews*, 2001, 222, 3-32; (b) C. D. Gutsche, *Calixarenes: an introduction*, Royal Society of Chemistry, 2008.
16. H. M. Keizer and R. P. Sijbesma, *Chemical Society reviews*, 2005, 34, 226-234.
17. (a) N. Morohashi, F. Narumi, N. Iki, T. Hattori and S. Miyano, *Chemical reviews*, 2006, 106, 5291-5316; (b) O. Kundrat, I. Cisarova, S. Böhm, M. Pojarova and P. Lhotak, *The Journal of Organic Chemistry*, 2009, 74, 4592-4596; (c) O. Kundrat, H. Dvorakova, V. Eigner and P. Lhotak, *The Journal of Organic Chemistry*, 2010, 75, 407-411; (d) O. Kundrat, H. Dvorakova, S. Böhm, V. Eigner and P. Lhotak, *The Journal of Organic Chemistry*, 2012, 77, 2272-2278; (e) Y. Bi, S. Du and W. Liao, *Coordination Chemistry Reviews*, 2014, 276, 61-72; (f) R. Kumar, Y. O. Lee, V. Bhalla, M. Kumar and J. S. Kim, *Chemical Society reviews*, 2014, 43, 4824-4870; (g) D.-S. Guo and Y. Liu, *Accounts of chemical research*, 2014, 47, 1925-1934.
18. H. Dvořáková, J. Lang, J. Vlach, J. Sýkora, M. Čajan, M. Himl, M. Pojarová, I. Stibor and P. Lhoták, *The Journal of Organic Chemistry*, 2007, 72, 7157-7166.
19. F. Hamada, M. Yamada, Y. Kondo, S.-i. Ito and U. Akiba, *CrystEngComm*, 2011, 13, 6920.
20. M. Yamada, Y. Ootashiro, Y. Kondo and F. Hamada, *Tetrahedron Letters*, 2013, 54, 1510-1514.
21. W. Wang, S. L. Gong, Y. Y. Chen and J. P. Ma, *New Journal Of Chemistry*, 2005, 29, 1390-1392.
22. (a) Y. Li, W. P. Yang, Y. Y. Chen and S. L. Gong, *Crystengcomm*, 2011, 13, 259-268; (b) Y. Li, W. P. Yang, R. Guo, Y. Y. Chen and S. L. Gong, *Crystengcomm*, 2012, 14, 1455-1462; (c) Y. Li, R. Guo, W. Wang, L. Gong, Y. Chen and S. Gong, *Wuhan Univ. J. Nat. Sci.*, 2013, 18, 300-306.
23. W. Yang, W. Wang, R. Guo, L. Gong and S. Gong, *Eur J Org Chem*, 2012, 2012, 3326-3330.
24. (a) G. M. Sheldrick, *SHELXL-97, A Program for Crystal Structure Solution*, University of Göttingen, Germany, 1997; (b) G. M. Sheldrick, *SHELXL-97, A Program for Crystal Structure Refinement*, University of Göttingen, Germany, 1997; (c) G. M. Sheldrick, *Acta crystallographica. Section A, Foundations of crystallography*, 2008, 64, 112-122.
25. L. J. Farrugia, *Journal of Applied Crystallography*, 1999, 32, 837-838.

Cite this: DOI: 10.1039/c0xx00000x

www.rsc.org/xxxxxx

ARTICLE TYPE

Table.2 Crystallographic data and structure correction parameters of the six compounds

Compound	**7·$CHCl_3$**	**8**	**9**	**10·H_2O**	**11**	**12·$CHCl_3$**
CCDC number	1056803	1056804	1056805	867095	867096	1056806
Formula	$C_{31}H_{28}O_5S_4$ ·0.17($CHCl_3$)	$C_{32}H_{28}O_6S_4$	$C_{33}H_{28}O_7S_4$	C_{40} H_{24} O_{24} S_4·H_2O	$C_{30}H_{22}O_7S_4$	6($C_{32}H_{26}O_4N_2S_4$) ·10($CHCl_3$)
Mr /g mol^{-1}	628.90	636.78	664.79	780.85	622.69	4978.4
Crystal system	Trigonal	Trigonal	Trigonal	Trigonal	Trigonal	Trigonal
Space group	$R\bar{3}$	$R\bar{3}$	$R\bar{3}$	$R\bar{3}$	$R\bar{3}$	$P\bar{3}$ $c1$
a/Å	36.329(5)	36.0289(13)	37.498(5)	25.766(4)	37.589(3)	23.994(6)
b/Å	36.329(5)	36.0289(13)	37.498(5)	25.766(4)	37.589(3)	23.994(6)
c/Å	11.8166(16)	12.2533(13)	11.9203(15)	29.978(6)	10.6810(16)	11.648(5)
α/°	90.00	90.00	90.00	90.00	90.00	90.00
β/°	90.00	90.00	90.00	90.00	90.00	90.00
γ/°	120.00	120.00	120.00	120.00	120.00	120.00
V [Å ^{3}]	13506(3)	13774.8(16)	14515(3)	17236(6)	13070(3)	5807(4)
Z	18	18	18	18	18	1
T/K	100(2)	173(2)	298(2)	293(2)	100(2)	296(2)
ρ_{calcd} /gcm^{-3}	1.365	1.382	1.369	1.351	1.417	1.424
μ/mm^{-1}	0.370	0.354	0.341	0.303	0.374	0.629
F (000)	5793	5976	6228	7236	5742	2548
θ range/°	1.84-25	2.99-25.36	1.82-25.69	2.28-28.00	1,877-31	1.7-25.00
Reflns collected/ unique	31597/5286 (R_{int}=0.0291)	13270/5439 (R_{int}=0.0837)	39803/6121 (R_{int}=0.0376)	32138/9248 (R_{int}=0.0399)	35903/9252 (R_{int}=0.0380)	23834/3427 (R_{int}=0.1164)
GOF	1.120	1.010	1.086	0.989	1.023	1.375
Final (I> 2σ(I)	R_1= 0.0753 wR_2= 0.2209	R_1= 0.0492 wR_2= 0.0804	R_1= 0.0628 wR_2= 0.1609	R_1= 0.0834 wR_2= 0.2569	R_1= 0.0802 wR_2= 0.2212	R_1= 0.1262 wR_2= 0.3612
Final indices (all data)	R_1= 0.0827 wR_2= 0.2301	R_1= 0.1244 wR_2= 0.0972	R_1= 0.1027 wR_2= 0.2089	R_1= 0.1360 wR_2= 0.2932	R_1= 0.1050 wR_2= 0.2377	R_1= 0.2083 wR_2= 0.4332

.